Supporting Information

Honeycomb-structured copper indium sulfide thin films obtained via a nanosphere colloidal lithography method

Efthymia Vakalopoulou[a], Thomas Rath[a,*], Fernando Gustavo Warchomicka[b], Francesco Carraro[c], Paolo Falcaro[c], Heinz Amenitsch[d], Gregor Trimmel[a]

[a] Institute for Chemistry and Technology of Materials, NAWI Graz, Graz University of Technology, Stremayrgasse 9, 8010 Graz, Austria

[b] Institute of Materials Science, Joining and Forming, Graz University of Technology, Kopernikusgasse 24, 8010, Graz, Austria

[c] Institute of Physical and Theoretical Chemistry, NAWI Graz, Graz University of Technology, Stremayrgasse 9, 8010 Graz, Austria

[d] Institute of Inorganic Chemistry, NAWI Graz, Graz University of Technology, Stremayrgasse 9, 8010 Graz, Austria

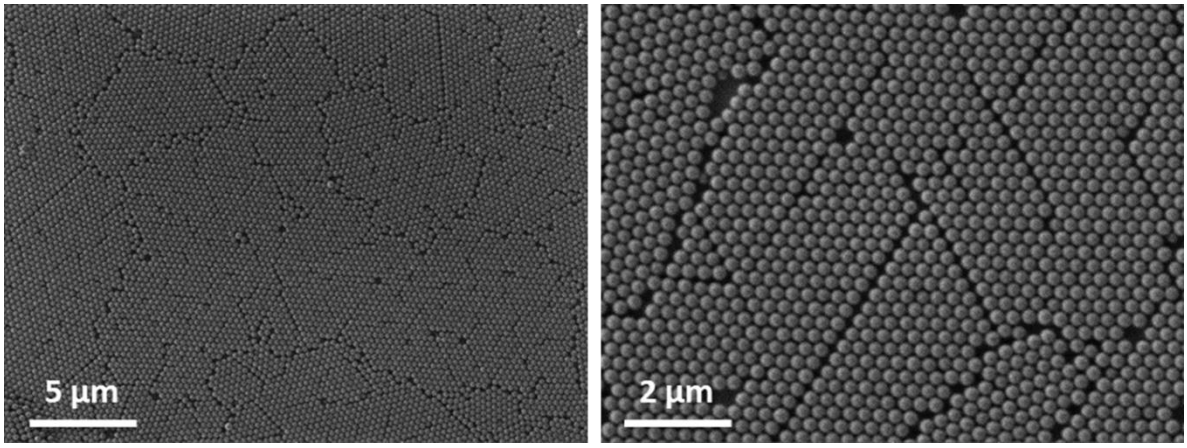

Figure S1. SEM images of the PS-MS templates prepared with an air/liquid interface method in two different magnifications.

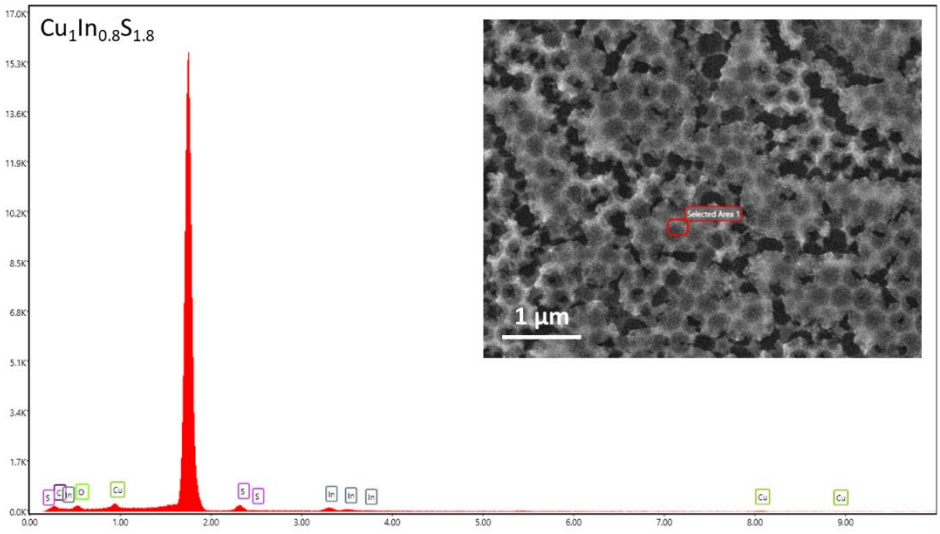

Element	Atomic %
C K	44.1
O K	43.5
S K	5.7
InL	2.4
CuK	3.2

Figure S2. EDX spectrum obtained from the CIS-P600 sample after annealing at 400 °C. The measurement was performed directly on the film.

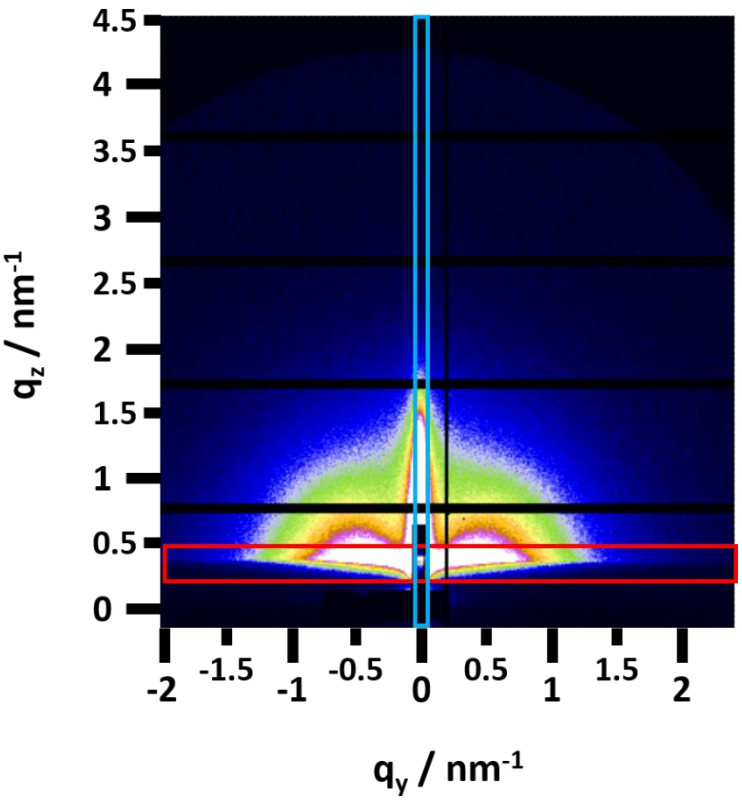

Figure S3. Analysis of the GISAXS data; the blue and red boxes enclose the out-of-plane and in-plane integration areas, respectively.

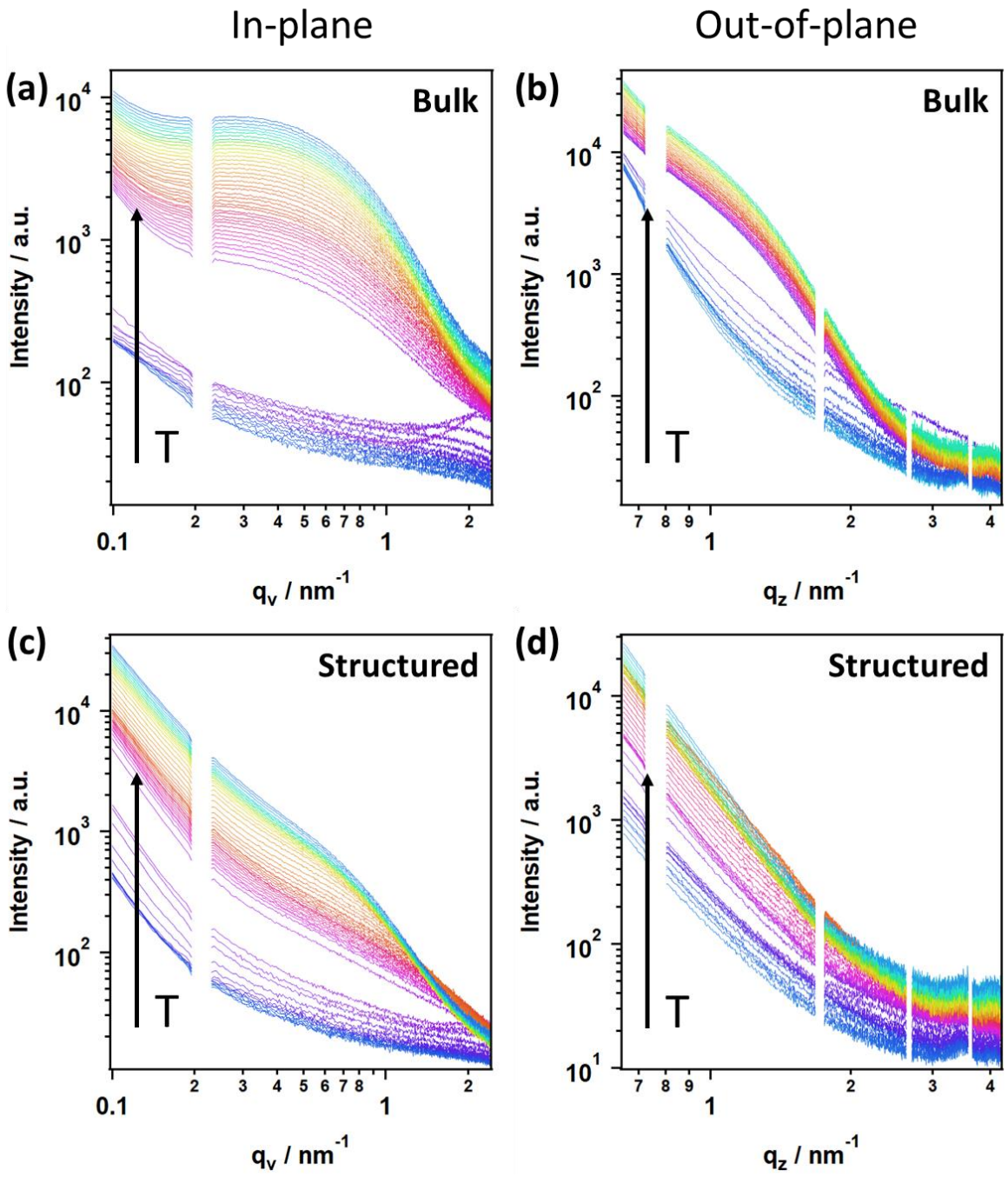

Figure S4. Temperature-dependent development of the **(a)** in-plane and **(b)** out-of-plane GISAXS patterns of the bulk film (non-structured) and temperature-dependent development of the **(c)** in-plane and **(d)** out-of-plane GISAXS patterns of the structured film. The increasing temperature (T) is indicated with a black arrow in the graphs. The data are shifted vertically for better visibility.

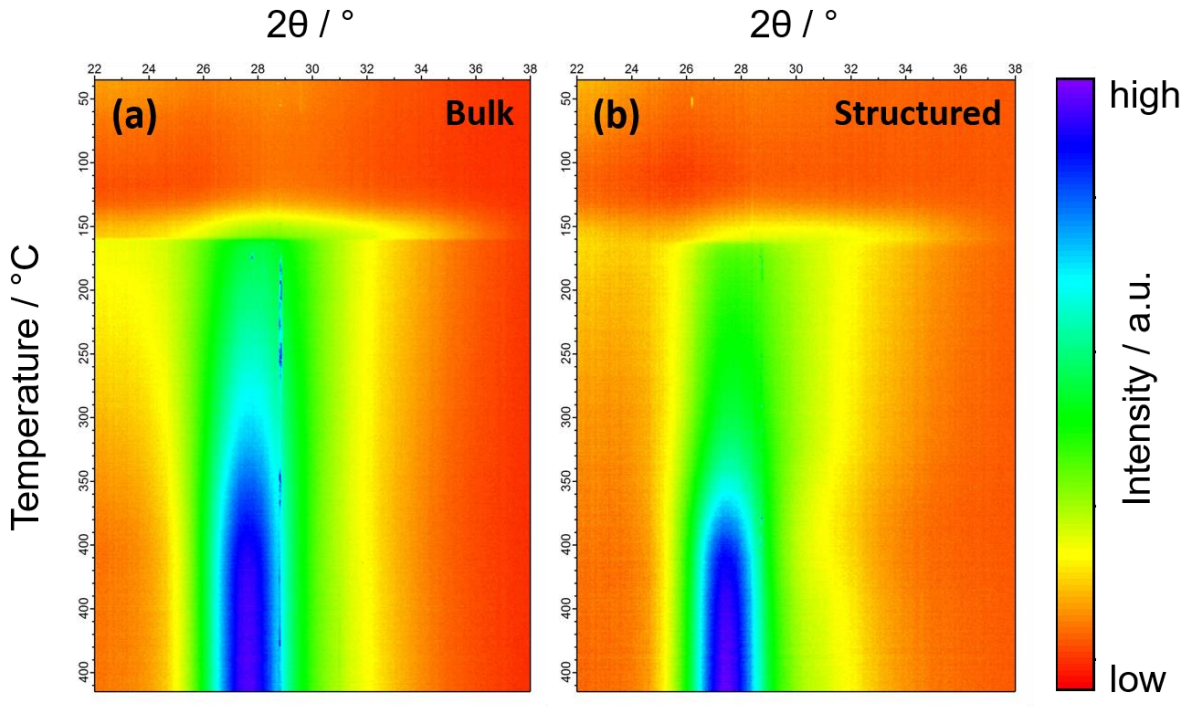

Figure S5. GIWAXS surface plots of **(a)** a bulk and **(b)** a structured film measured between 22 and 38° 2θ during heating runs from 35 up to 400 °C with a heating rate of 10 °C/min and a subsequent annealing time of 15 min at 400 °C.

Determination of the Porod invariant and correlation length

As a sensitive estimate of changes related to the mass as well as the shape of the scattering pattern, the Porod invariant **Q** and the correlation length $\mathbf{l_{corr}}$ have been calculated, respectively, by integrating the scattering pattern over the accessible q-range in the in-plane direction derived by averaging the masked image (Figure S3) with:

$$Q = \int_{q_{min}}^{q_{max}} dq_h \; {q_h}^2 \, I(q_h)$$

and

$$l_{cor} = {\pi}/{Q} \int_{q_{min}}^{q_{max}} dq_h \; q_h \, I(q_h)$$

$I(q_h)$ denotes the scattering pattern (in-plane), q_{min} / q_{max} the minimum and maximum q-values and q_h the q-axis (in-plane).

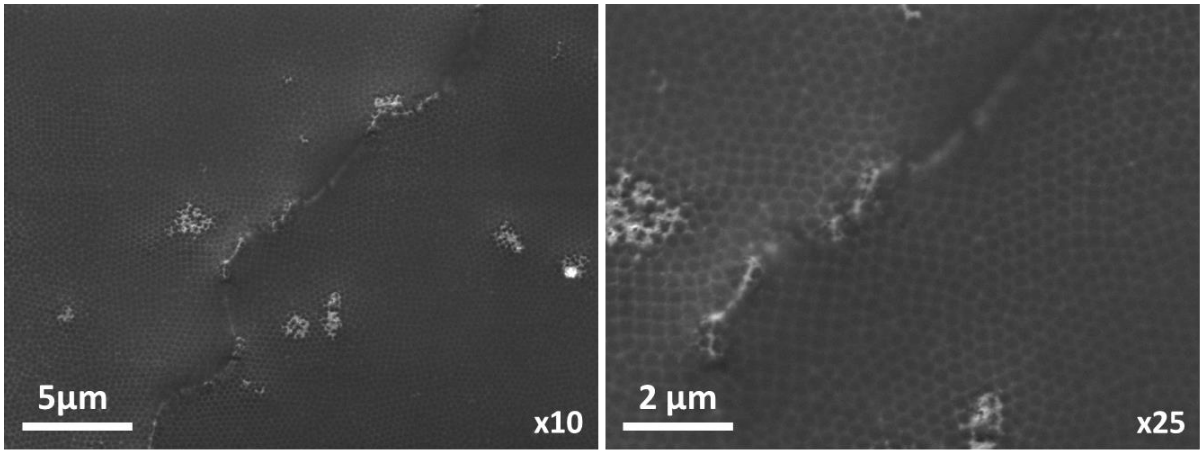

Figure S6. SEM images after the infiltration of the PS-NS template and conversion of the metal xanthates to $CuInS_2$ at 195 °C.

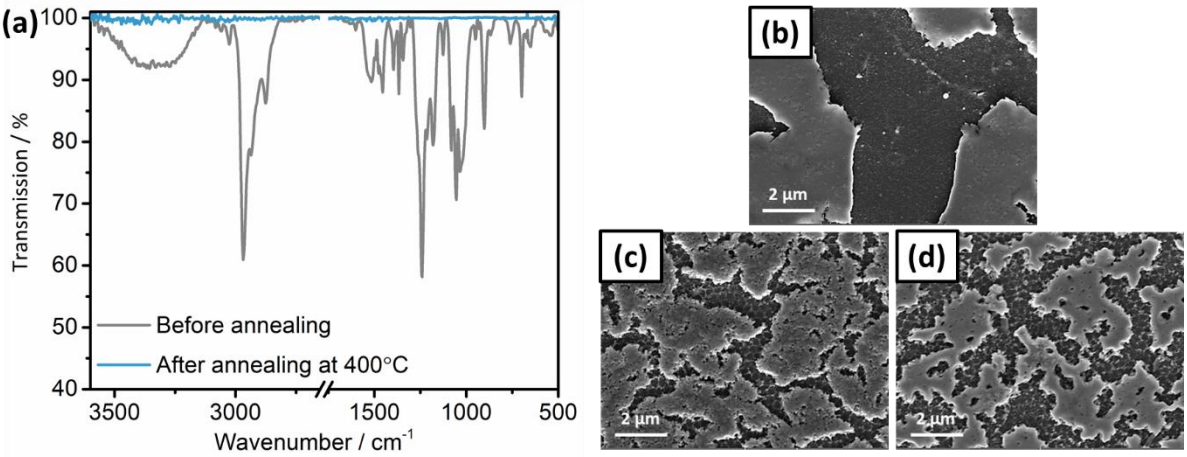

Figure S7. (a) FT-IR spectra after infiltration of the PS-NS template with the precursor solution (grey) and after annealing at 400 °C (blue) of initial attempts using a too high precursor concentration. SEM images of **(b)** CIS-P0, **(c)** CIS-P300 and **(d)** CIS-P600 after annealing at 400 °C.

Alternative template removal strategies

Annealing at 280 °C in air: The high temperature treatment for the template removal, used in the described approach, could be a limiting factor for some applications. Thus, we evaluated the possibility of applying a lower temperature based on the fact that polystyrene can undergo a thermal oxidation at lower temperatures in presence of air.[1] This has method has been already used for the removal of the PS-NS in the formation of hexagonally-structured TiO_2 and SiO_2.[2] Therefore, we followed a similar procedure and subjected the samples to thermal oxidation at 280 °C after the formation and infiltration of the P300 and P600 samples (the P0 sample was not used, as it was not possible to obtain honeycomb structures with this sample). The FT-IR spectra in Figure S8 show that after the oxidation, there are no vibration bands visible, which would correspond either to the xanthates or to polystyrene. Additionally, the SEM images display the desired honeycomb structures. The question stemming from the thermal oxidation, however, was to which extent the oxygen presence can influence the decomposition of the xanthates and hence the formation of $CuInS_2$. EDX analyses, of the prepared films show an elemental ratio of 1:1.1:0.3 for Cu, In and S (Figure S9). This ratio does not fit to the stoichiometric ratio of $CuInS_2$ and leads to the outcome that partial oxidation of the copper indium sulfide has occurred and hence this procedure of template removal is not suitable.

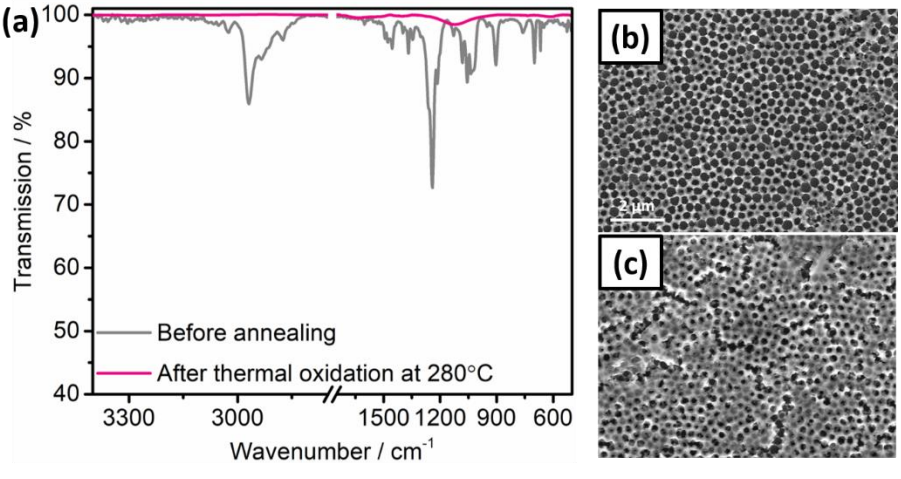

Figure S8. (a) FT-IR spectra after infiltration of the PS-NS template with the precursor solution (grey) and after the thermal oxidation process at 280 °C (pink). SEM images of **(b)** CIS-P300 and **(c)** CIS-P600 after thermal oxidation at 280 °C.

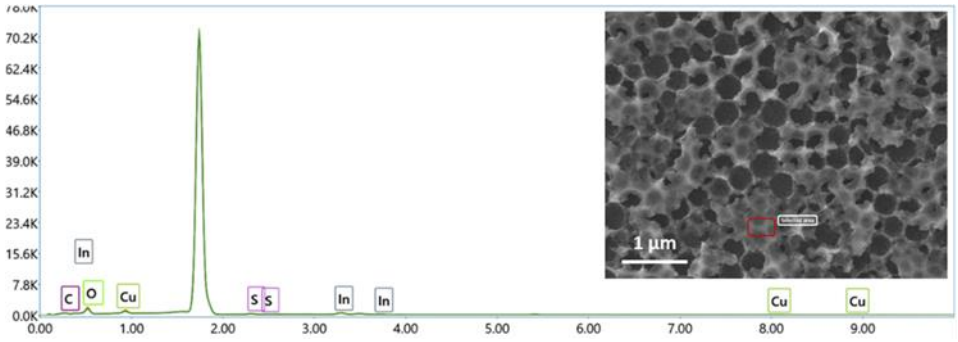

Element	Atomic %
C K	35.7
O K	55.1
S K	1.1
InL	4.3
CuK	3.8

Figure S9. EDX spectrum obtained from the CIS-P600 sample after thermal oxidation at 280 °C. The measurement was performed directly on the film.

Dissolution of PS nanospheres after the formation of $CuInS_2$ at 195 °C: The initial steps of infiltration and $CuInS_2$ formation were kept as described before, but instead of heating the system under conditions in which the polystyrene is decomposed, the thermal process was performed under inert conditions and stopped at 195 °C, where only the conversion of the xanthates to the $CuInS_2$ occurs. Subsequently, these films were soaked in chloroform for 24 h in order to dissolve the PS-NS template. However, the polystyrene dissolution was not successful, as the vibrations of PS are still present in the FT-IR spectra after this procedure (Figure S10). The intensity after 24 h soaking is only slightly decreased, indicating the partial dissolution of the polystyrene. Based on this observation, we can suggest two reasons for such an outcome. Firstly, the chemical decomposition of the xanthates – either by the high temperature or by side reactions - can potentially cause cross-linking reactions, which make the polystyrene insoluble in common solvents. Secondly, the O_2 plasma etching is known that it can create oxygen-based groups on the polymer due to the reactive oxygen radicals that are formed under the plasma conditions.[3] This, in combination with the high temperatures occurring during the xanthate decomposition, can potentially cause crosslinking reactions leading to the insolubility of the polystyrene.

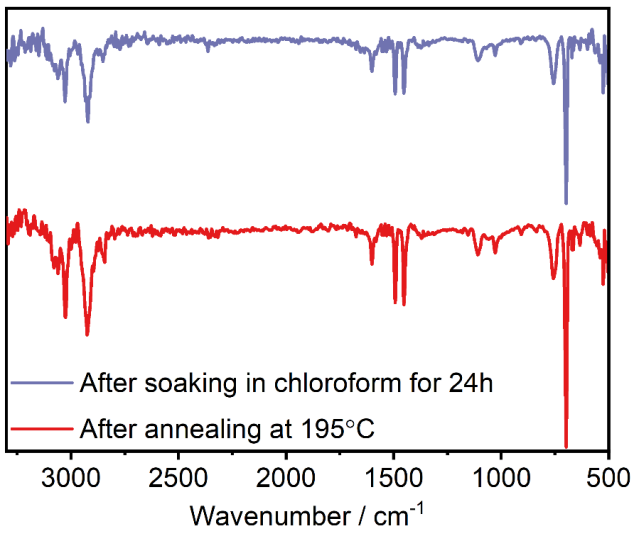

Figure S10. FT-IR spectra of films after annealing at 195 °C (lower spectrum) and after soaking of the sample in chloroform for 24 h, for PS-MS template dissolution (upper spectrum). The spectra are shifted vertically for better visibility.

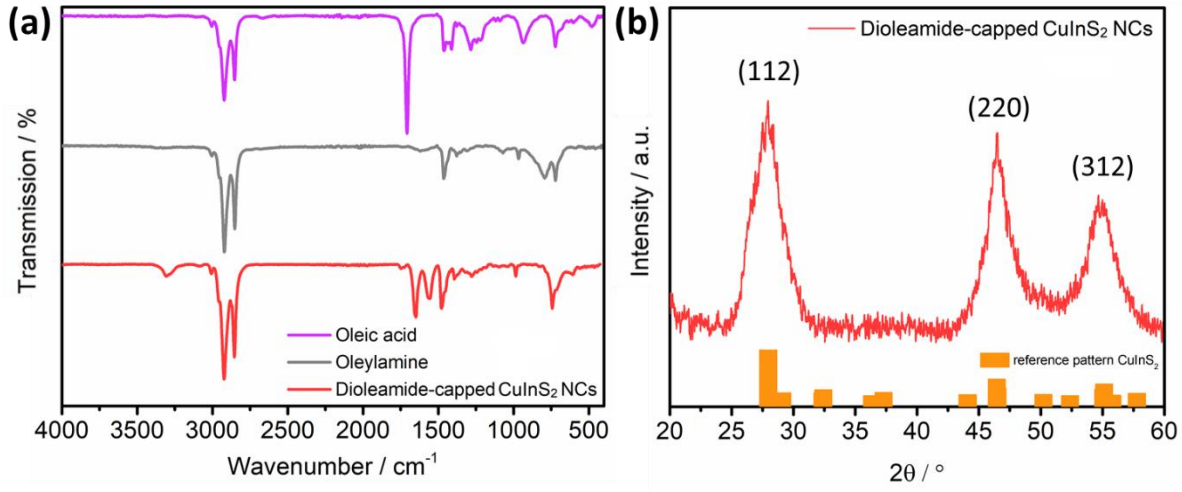

Figure S11. (a) FT-IR spectra of dioleamide-capped $CuInS_2$ NCs (red spectrum), free oleylamine (grey spectrum) and free oleic acid (purple spectrum). The spectra are shifted vertically for better visibility. **(b)** X-ray diffraction pattern of $CuInS_2$ before ligand exchange, with a reference pattern for chalcopyrite $CuInS_2$ (ICSD-42127).

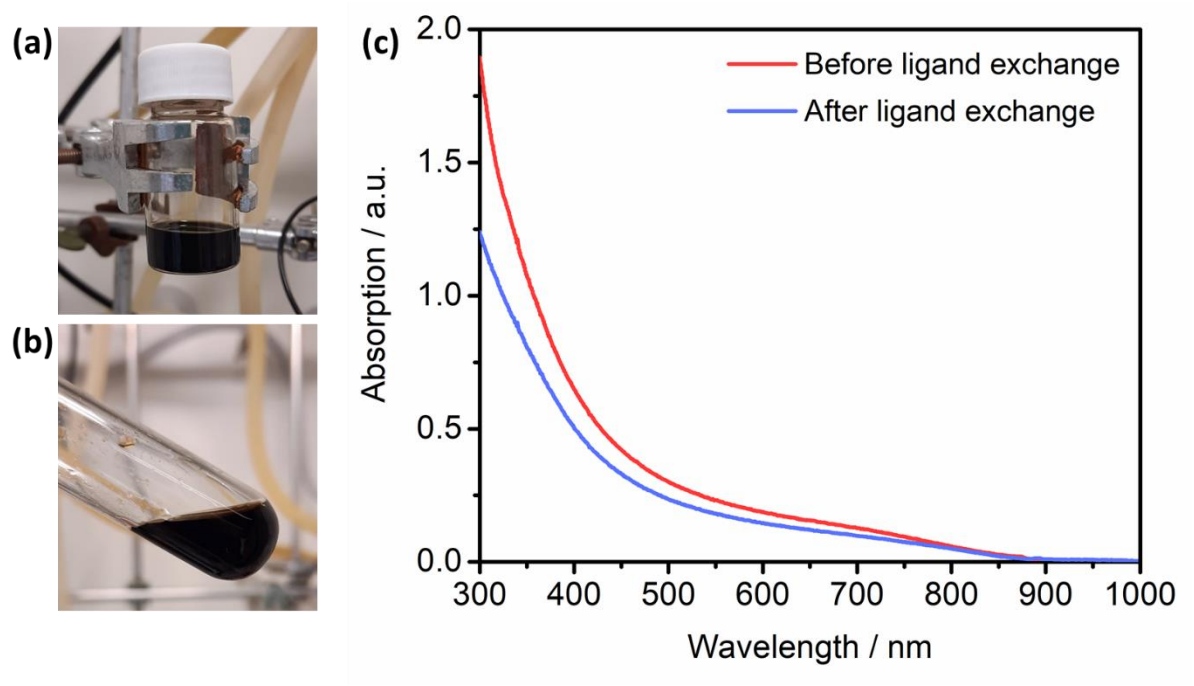

Figure S12. Digital photos of the **(a)** dioleamide-capped $CuInS_2$ nanocrystals dispersed in toluene and **(b)** thioglycerol-capped $CuInS_2$ nanocrystals dispersed in DMSO. **(c)** UV-Vis spectra of the $CuInS_2$ nanocrystals before and after ligand exchange.

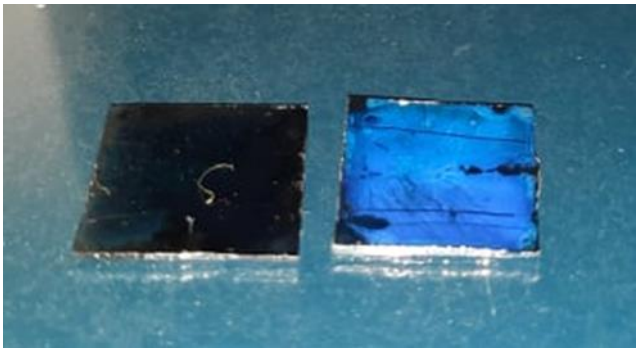

Figure S13. Digital photo of the films before (left) and after (right) template removal (nanocrystal ink route).

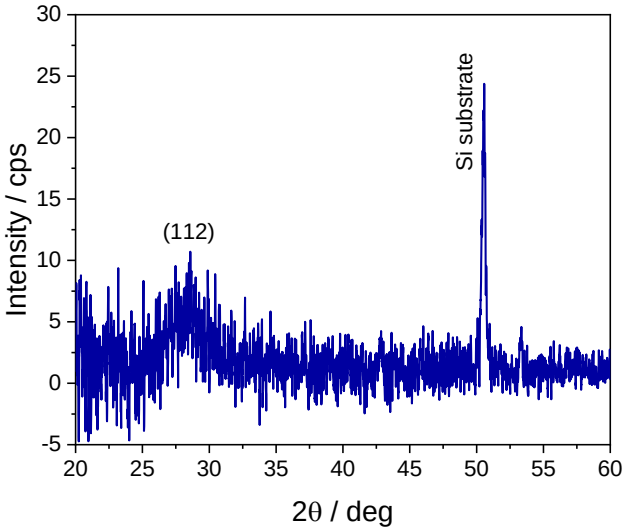

Figure S14. GIXRD pattern of a 75 nm thick honeycomb structured $CuInS_2$ film on a silicon substrate prepared via the nanocrystal ink route.

References

1 P. Pfäffli, A. Zitting and H. Vainio, *Scand. J. Work. Environ. Health*, 1978, **4**, 22–27.

2 M. T. Hörantner, W. Zhang, M. Saliba, K. Wojciechowski and H. J. Snaith, *Energy Environ. Sci.*, 2015, **8**, 2041–2047.

3 D. E. Frank, *Pure Appl. Chem.*, 1990, **62**, 1699–1708.